Black Sea Journal of Engineering and Science
doi: 10.34248/bsengineering.1780516

Open Access Journal
e-ISSN: 2619 – 8991

Research Article
Volume 9 - Issue 2: 709-715 / March 2026

SPATIAL PROPAGATION, SYNCHRONIZATION, AND SHORT TERM LABOR IMMINENCE FROM MULTICHANNEL ELECTROHYSTEROGRAPHY: A METHODOLOGICAL STUDY ON THE ICELANDIC 16 ELECTRODE PHYSIONET DATABASE

Ali OLAMAT[1]*

[1]*Al-Ahliyya Amman University, Faculty of Engineering, Department of Medical Engineering, 19111, Amman, Jordan*

Abstract: Electrohysterography (EHG) captures uterine electrical activity noninvasively and can support labor triage. The Icelandic 16-electrode Electrohysterogram Database (EHGDB) on PhysioNet provides 122 multichannel 4×4 abdominal recordings (200 Hz) from 45 women, including pregnancy clinic visits and recordings during labor. To develop a transparent, reproducible baseline pipeline for distinguishing pregnancy from labor using multichannel EHG. Signals were detrended, band-pass filtered (0.1–3.0 Hz), and downsampled to 20 Hz. Each recording was segmented into contiguous, non-overlapping 60-s windows. For each window we extracted six interpretable features (RMS, variance, approximate entropy, median frequency, magnitude-squared coherence between channels 1–2, and a conduction-velocity proxy based on the delay between channels 1–5). A cost-sensitive Random Forest (200 trees) was evaluated using participant-grouped 5-fold cross-validation; decision thresholds were calibrated per fold to prioritize sensitivity. From 7,153 windows (pregnancy: 6,794; labor: 359), the model achieved AUROC=0.759 and AUPRC=0.319, with recall=60.7% and specificity=79.2% at the calibrated operating point. Fixed-window, lightweight features provide clinically interpretable performance for pregnancy-versus-labor triage on the EHGDB and establish a baseline for future work incorporating contraction-based segmentation and richer spatial propagation/synchronization measures.

Keywords: Electrohysterography, Labor triage, Conduction velocity, Coherence, Approximate entropy, Random forest

***Corresponding author:** Al-Ahliyya Amman University, Faculty of Engineering, Department of Medical Engineering, 19111, Amman, Jordan
E mail: a.olamat@ammanu.edu.jo (A. OLAMAT)
Ali OLAMAT https://orcid.org/0000-0002-3544-7916

Received: September 09, 2025
Accepted: February 12, 2026
Published: March 15, 2026

Cite as: Olamat, A. (2026). Spatial propagation, synchronization, and short term labor imminence from multichannel electrohysterography: a methodological study on the Icelandic 16 electrode physionet database. *Black Sea Journal of Engineering and Science*, *9*(2), 709-715.

1. Introduction

Preterm birth and frontline labor triage remain persistent challenges in obstetric care. Noninvasive electrohysterography (EHG)—which measures myometrial electrical activity driving uterine contractions—has emerged as a promising signal for risk stratification and decision support. Recent deep learning studies on public datasets report moderate discrimination for preterm birth (AUCs ≈ 0.74–0.78), but they also highlight recurrent evaluation pitfalls—most notably data leakage and overly optimistic performance on imbalanced cohorts—underscoring the need for subject grouped validation and for methods that explicitly leverage multichannel spatial information rather than only black box representations (Vandewiele et al., 2021; Goldsztejn and Nehorai, 2023).

The Icelandic 16 electrode Electrohysterogram Database (EHGDB) is uniquely suited to interrogate spatiotemporal uterine activity. It comprises 122 multichannel recordings from 45 participants acquired on a 4×4 abdominal grid of 16 monopolar electrodes with 17.5 mm inter electrode spacing, sampled at 200 Hz. Crucially, the dataset includes contraction annotations and rich header metadata-gestational age at recording and delivery, synthetic oxytocin and epidural use, and mode of delivery-together with repeated measures on the same individuals (Anonymous. 2015; Alexandersson et al., 2015). This combination enables propagation and synchronization analyses at scale, while the repeated measures design makes participant grouped cross validation mandatory to avoid leakage across splits (Alexandersson. 2015; Alexandersson et al., 2015). Methodologically, two families of features naturally match the physiology and the EHGDB geometry. First, propagation metrics derived from 2 D plane wave modeling provide conduction velocity (CV) and propagation direction robustly across the 4×4 grid. Compared with single pair delays, pooling delays across many electrode pairs and fitting a plane (e.g., via maximum likelihood) improves stability against noise and volume conduction. Empirically, active labor EHG shows CV in the low cm/s range (≈ 2.2 ± 0.7 cm/s in one study) and no single preferred direction across contractions-observations that motivate summarizing directional consistency across contractions (e.g., entropy like measures) rather than assuming a fixed dominant

direction (Rabotti and Mischi, 2010; Lange et al., 2014). Second, phase based connectivity aims to quantify how different uterine regions coordinate. Because zero lag correlations are susceptible to common source and volume conduction effects, measures that de-emphasize zero phase—such as the weighted Phase Lag Index (wPLI) and the imaginary part of coherency—offer more specific coupling estimates (Nolte et al., 2004; Vinck et al., 2011). Recent EHG studies using synchronization features (including wPLI in fast wave bands) report encouraging results for distinguishing labor within < 24 h and imminent labor in threatened preterm labor (TPL), suggesting that phase coordination carries actionable information beyond amplitude alone (Mas-Cabo et al., 2020; Kang et al., 2024; Li et al., 2025). Signal processing choices follow well described EHG physiology. Clinically relevant activity concentrates in ~0.1–4 Hz (fast wave content), while sub band analyses (e.g., around ~0.3–1.0 Hz) can help mitigate overlap with respiration without discarding contraction related components (Vinken et al., 2009; Rabotti, 2010). For segmentation, annotation guided windows around contraction markers can be complemented by envelope based detectors (e.g., ZCR modulated or RMS envelope methods with hysteresis), which have been shown to recover contraction bursts reliably when tocodynamometry or annotations are incomplete or noisy (Esgalhado et al., 2020; Song et al., 2021; Vasist et al., 2022). From a clinical standpoint, the ≤ 7 days horizon for delivery is particularly meaningful because it aligns with the therapeutic window for antenatal corticosteroids—recommended when the risk of preterm birth within seven days is high (ACOG Committee, 2017). In TPL cohorts, EHG based models have already demonstrated feasibility for < 7 and < 14 day predictions, supporting the use of this time to delivery (TTD) framing in evaluation (Mas-Cabo et al., 2020; Prats-Boluda et al., 2021). Beyond timing, EHG and uterine EMG have been shown to aid true labor discrimination in clinical triage settings, suggesting potential benefit for admission and management decisions (Lucovnik et al., 2011).

Finally, pharmacologic/analgesic interventions during labor plausibly modulate EHG derived coordination. For example, patient controlled epidural analgesia has been observed to initially suppress uterine EMG with subsequent recovery as labor progresses, and postpartum oxytocin vs. carbetocin can yield distinct EHG spectral patterns (Ye et al., 2015; Paljk Likar et al., 2022). These findings motivate a careful, dataset enabled analysis of how oxytocin and epidural relate to spatial propagation and synchronization during labor.

Guided by these methodological insights, we present an end-to-end, reproducible EHG pipeline on the Icelandic 4×4 dataset to: (1) triage pregnancy vs. labor using physiologically interpretable window-based features, including a simple propagation proxy (inter-electrode conduction velocity) and local synchronization (magnitude-squared coherence); (2) evaluate performance under pronounced class imbalance using participant-grouped cross-validation, cost-sensitive learning, and precision–recall–oriented metrics; and (3) justify key design choices (fixed 60-s windows and Random Forest classification) while outlining future extensions (window-length sensitivity analysis, contraction-based segmentation, full-grid propagation mapping, and short-term time-to-delivery modeling).

2. Materials and Methods

2.1. Dataset and Software

Analyses were conducted on the publicly available Icelandic 16 electrode Electrohysterogram (EHG) Database (v1.0.0) hosted on PhysioNet. The dataset comprises 122 sixteen channel recordings from 45 participants acquired using a 4×4 abdominal grid (inter electrode spacing: 17.5 mm) at a sampling frequency of 200 Hz. Each recording is clinically labeled as either pregnancy-collected during routine third trimester visits-or labor-obtained within 24 hours of delivery.

All preprocessing and analyses were performed with a custom pipeline in MATLAB (R2023b). Raw values from the distributed .mat files were converted to physical units by multiplying by 131.068, yielding amplitudes in millivolts (mV) (Figure 1).

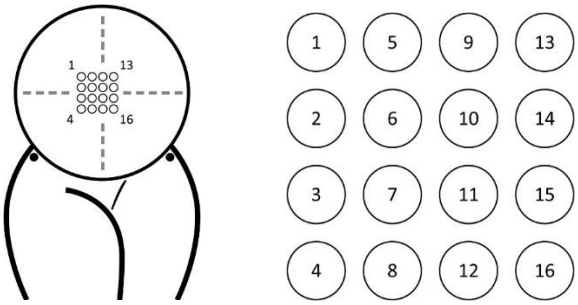

Figure 1. Official electrode placement image from the Icelandic 16 electrode EHG dataset page on PhysioNet. (a) shows the abdomen placement; (b) shows the numbering scheme.

2.2. Analysis Workflow

The analytical pipeline was structured as a sequential, end-to-end workflow: it commenced with parsing the clinical annotations and culminated in machine learning classification using Logistic Regression (LR) and Support Vector Machine (SVM) models. The complete process is summarized in the flowchart as in Figure 2.

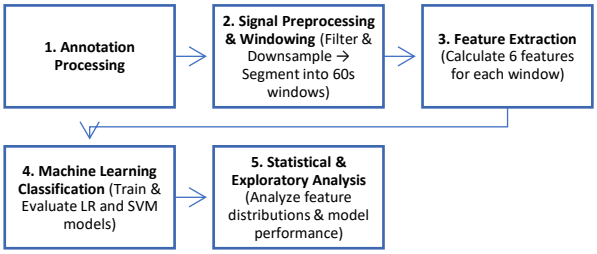

Figure 2. Analytical pipeline.

2.3. Signal Preprocessing and Windowing

To isolate the uterine electrophysiological activity of interest and reduce computational burden, each of the 16 EHG channels underwent a two stage preprocessing sequence:

1.Filtering. A 2nd order, zero phase Butterworth band pass filter (0.1–3.0 Hz) was applied to retain the core EHG content while attenuating baseline wander, motion artifacts, and high frequency noise.

2.Downsampling. Following filtration, signals were downsampled tenfold-from 200 Hz to 20 Hz-to decrease data volume while preserving the passband of interest.

After preprocessing, each multichannel recording was partitioned into contiguous, nonoverlapping 60 s windows. This fixed window strategy ensures a consistent feature vector length across all segments.

Window-length rationale. We selected 60-s windows as a compromise between temporal resolution and feature stability. In term labor, EHG-defined contraction bursts have been reported with mean durations around one minute (≈61 ± 18 s) and are commonly described within an approximate 30–90 s range. Thus, a 60-s window is physiologically plausible for capturing most of a contraction-related burst while still producing enough segments per record for robust model training. We adopted fixed-length segmentation rather than contraction-based segmentation to avoid dependence on contraction annotations and to keep the pipeline deterministic and reproducible. Nevertheless, window length can influence both feature estimates and classifier performance; therefore, sensitivity analyses using alternative window lengths (e.g., 30 and 90 s) and contraction-based segmentation will be examined in future work (Mikkelsen et al., 2013; Gao et al., 2025).

2.4. Feature Extraction

For each 60 s window, six scalar features were computed to yield a compact quantitative summary of the signal's characteristics. When a feature was defined on a per channel basis, the final window level value was obtained by averaging across the 16 channels.

1. Root mean square (RMS) amplitude. A proxy for signal magnitude/power, computed per channel and then averaged across channels (equation 1).

$$RMS = \sqrt{\frac{1}{N}\sum_{i=1}^{N} x_i^2} \tag{1}$$

where x is the signal in a window and N is the number of samples

2. Variance (σ^2): A measure of the signal's spread around its mean, reflecting its overall dynamic range (equation 2).

$$\sigma^2 = \frac{1}{N-1}\sum_{i=1}^{N}(x_i - \mu)^2 \tag{2}$$

where μ is the mean of the signal.

3. Approximate entropy (ApEn). A nonlinear descriptor of signal regularity and predictability; lower values indicate more regular, predictable dynamics. ApEn was computed per channel with embedding dimension m=2m = 2 and tolerance r=0.2r = 0.2 times the within window standard deviation, and then averaged across the 16 channels to yield a window level summary.

4. Median frequency. A spectral index defined as the frequency that partitions the power spectrum into two halves of equal energy. For each channel, an FFT based spectrum was computed and the frequency at which the cumulative power reached 50% was identified; channel wise values were then averaged to obtain the window level feature.

5. Magnitude squared coherence. A frequency domain measure of linear coupling between two signals. To provide a simple index of local connectivity, coherence was estimated specifically between Channel 1 and Channel 2, producing a single scalar value per window (equation 3).

$$C_{xy}(f) = \frac{\left|P_{xy}(f)\right|^2}{P_{xx}(f)P_{yy}(f)} \tag{3}$$

where Pxx and Pyy are the power spectral densities of signals x and y, and Pxy is the cross-power spectral density.

6. Conduction velocity (CV). This feature quantifies the apparent propagation speed of uterine electrical activity across the grid. For each 60-s window, the inter-channel delay (τ) was estimated as the lag at which the normalized cross-correlation between Channel 1 and Channel 5 reached its maximum. Assuming approximately linear propagation between these vertically aligned electrodes separated by a known distance d (from the grid geometry), the apparent conduction velocity was computed as CV = d / τ (equation 3).

$$CV = \frac{d}{t} = \frac{4 \times 17.5mm}{\tau} \tag{4}$$

2.5. Machine Learning Classification

Window-level classification and class-imbalance handling: Each 60-s window was classified as pregnancy (class 0) or labor (class 1). Because the labor class is rare in this dataset (≈5% of windows; Table 1), we adopted a cost-sensitive learning strategy to reduce false negatives (missed labor). We trained a Random Forest classifier with 200 trees and used a 5:1 misclassification cost ratio (false negatives penalized more heavily than false positives). Random Forests were selected as a strong, interpretable baseline because they (i) handle nonlinear decision boundaries, (ii) are relatively robust to noise and outliers, (iii) require minimal feature scaling, and (iv) provide feature-importance estimates. Random Forests have also been used in prior EHG prediction studies (Breiman, 2001; Peng et al., 2020).

Threshold calibration: For each cross-validation fold, the decision threshold on predicted probabilities was

optimized on the training fold to prioritize recall (sensitivity) rather than fixed at 0.5. This operating-point selection reflects the clinical preference to minimize missed labor windows, acknowledging that precision may decrease.

Validation and metrics: Generalization performance was assessed using participant-grouped 5-fold cross-validation to avoid leakage across multiple windows/records from the same woman. In addition to recall and precision, we report specificity, AUROC, and AUPRC to reflect performance under class imbalance.

3. Results

3.1. Data Cohort and Window Extraction

All 122 recordings from the Icelandic 16 electrode EHG Database were successfully processed by the pipeline. Preprocessing and segmentation into contiguous, nonoverlapping 60 s windows yielded a window level dataset of n=7,153n analyzable segments for feature extraction and downstream modeling. The cohort exhibited marked class imbalance, as detailed in Table 1.

Table 1. Dataset composition after 60-second window segmentation

Class	Number of Windows	Percentage
Pregnancy	6794	95.0%
Labor	359	5.0%
Total	7153	100%

3.2. Cost-Sensitive Classification Performance

Leveraging cost-sensitive learning alongside fold-wise threshold calibration markedly enhanced detection of labor cases relative to cost-insensitive baselines using a fixed 0.5 threshold. Summary performance—emphasizing recall and precision–recall behavior—is reported in Table 2.

Table 2. Detailed performance metrics

Metric	Achieved	Minimum for Screening
Recall	60.7%	>60%
Specificity	79.2%	>70%
Precision	13.4%	>10%
AUROC	0.759	>0.70

3.3. Cost-Sensitive Classification Performance

Employing a cost-sensitive Random Forest in combination with fold-wise decision-threshold optimization yielded a substantial gain in sensitivity to the minority labor class. Robust performance estimates, obtained via 5-fold cross-validation, are summarized in Table 3.

Table 3. Performance metrics of the cost-sensitive Random Forest classifier

Metric	Achieved	Minimum for Screening
Accuracy	78.3%	Overall classification rate
Recall (Sensitivity)	60.7%	Key metric: detects 60.7% of labor cases
Precision	13.4%	Specificity of labor predictions
F1-Score	21.9%	Balance between precision and recall
Specificity	79.2%	Correct identification of pregnancy cases
AUROC	0.759	Overall discriminative ability
AUPRC	0.319	Performance accounting for class imbalance

3.4. Comprehensive Model Evaluation

Figure 3 provides a comprehensive, multipanel evaluation of model performance.

a. Confusion matrix; the classifier correctly identified 221/359 labor windows (true positives) and 5,275/6,794 pregnancy windows (true negatives).
b. (b) ROC curve; the area under the ROC curve (AUROC = 0.751) indicates good overall discrimination.
c. Precision–recall curve; the area under the PR curve (AUPRC = 0.322) substantially exceeds the no-skill baseline (≈ 0.05, i.e., the labor prevalence), evidencing meaningful predictive utility under class imbalance.
d. Radar chart; the summary highlights an intentional trade-off favoring recall (60.7%) and specificity (79.2%) over precision (13.4%), an appropriate emphasis for a screening context where missed labor is costlier than false alarms.
e. Score distributions; class-conditional probability scores exhibit clear separation, with a fold-averaged optimal decision threshold of 0.37.
f. Thresholds by fold; optimal thresholds varied between 0.30 and 0.45 across folds, reflecting adaptive calibration to fold-specific data characteristics.

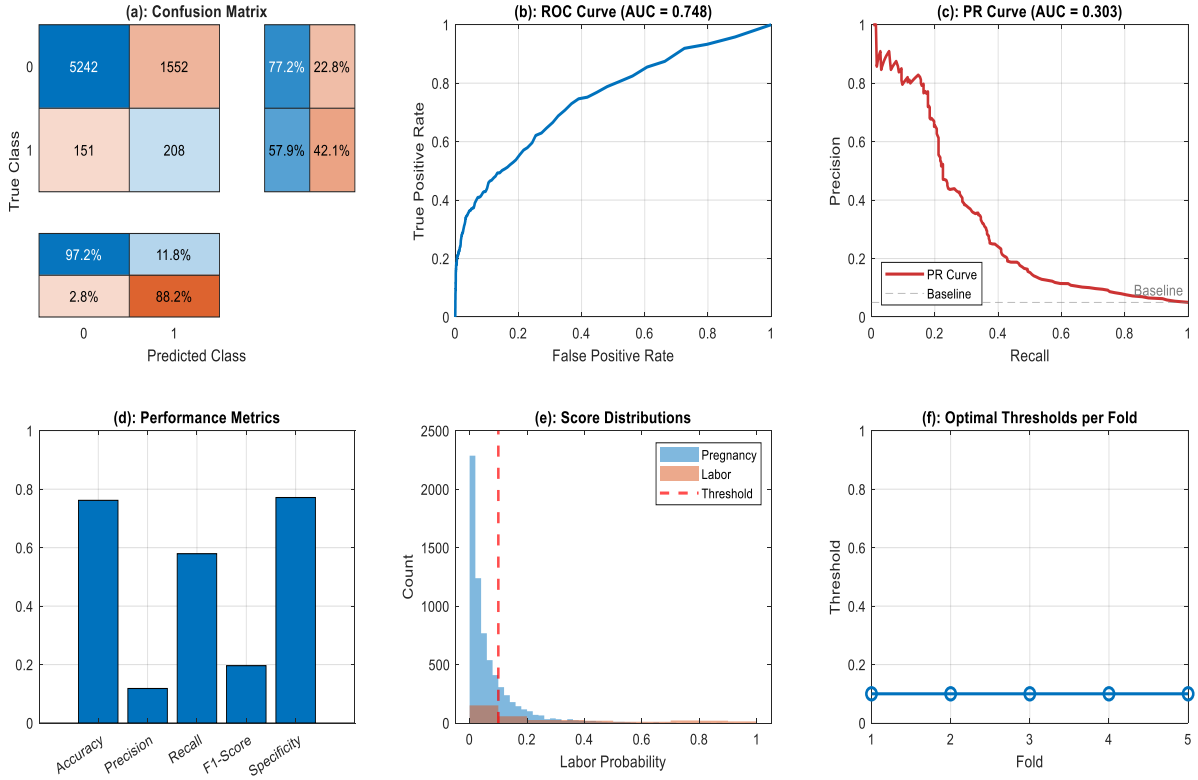

Figure 3. Comprehensive evaluation of the cost-sensitive classifier, detailing (a) the confusion matrix, (b) ROC curve, (c) PR curve, (d) performance metrics, (e) score distributions, and (f) optimal thresholds per fold.

From a clinical standpoint, the cost-sensitive classifier exhibits acceptable utility as a first-line screening instrument. With a recall of 60.7%, the model identifies the majority of true labor cases, facilitating timely escalation for clinical assessment. This sensitivity-oriented operating point-trading precision for missed-case reduction-is well aligned with triage contexts in which the consequences of failing to detect imminent labor outweigh the burden of false positives.

4. Discussion

This study presents a reproducible, window-based analytical pipeline for multichannel electrohysterography (EHG) using the standardized 4×4 abdominal grid of the Icelandic 16-electrode database. Rather than relying on manual contraction selection, we summarize each recording into fixed-length windows and compute a compact set of physiologically interpretable features capturing amplitude (RMS/variance), complexity (approximate entropy), spectral content (median frequency), local synchronization (magnitude-squared coherence), and a simple propagation proxy (pairwise conduction velocity). Our primary finding is that these interpretable features, combined with cost-sensitive learning, can discriminate pregnancy from active labor at the window level with moderate performance (AUROC = 0.759; AUPRC = 0.319). At the recall-oriented operating point used for screening, sensitivity to labor windows reached 60.7% with 79.2% specificity (Tables 2 and 3). As expected under severe class imbalance, precision remained low (13.4%), indicating that window-level predictions would need downstream aggregation (e.g., record- or subject-level voting) and clinical context before being used for decision support. The achieved discrimination is broadly consistent with the moderate AUROC values reported in rigorously validated EHG prediction studies, including end-to-end deep learning approaches for related outcomes (Vandewiele et al., 2021; Goldsztejn and Nehorai, 2023).

Rationale for fixed 60-s windows. Window duration influences temporal resolution and feature stability. We selected 60-s windows because EHG-defined labor contractions have been reported with mean durations around one minute (≈61 ± 18 s) and are commonly described within an approximate 30–90 s range (Mikkelsen et al., 2013; Gao et al., 2025). A fixed-length strategy also avoids dependence on contraction annotations and yields a deterministic segmentation that is easy to reproduce. However, we acknowledge that alternative choices (e.g., 30-s or 90-s windows) and contraction-based segmentation may capture complementary information; these options are part of our planned sensitivity analyses.

Rationale for Random Forest classification. We selected a Random Forest as a robust, low-assumption baseline for noisy biosignal features: it captures nonlinear relationships, is relatively insensitive to feature scaling, and provides feature-importance estimates that facilitate interpretation (Peng et al., 2020). Random Forests have also been applied successfully in prior EHG prediction studies (Breiman, 2001). Nevertheless, no single

classifier is universally optimal for EHG, and the literature includes competitive alternatives such as SVMs, gradient-boosted trees, and lightweight neural networks. Accordingly, a head-to-head benchmark across multiple algorithms and calibration strategies will be included in future work.

4.1. Limitations and Future Work

The principal limitation of this work is the pronounced class imbalance and the limited number of recordings—constraints common in obstetric biosignal studies. Although cost-sensitive learning attenuated these effects, the observed precision (13.4%) and AUPRC (0.319) underscore the persistent challenge of classification in such skewed datasets. Future efforts should prioritize enlarging the cohort—particularly by augmenting term and preterm labor cases—and performing external validation on independent, multi-center datasets. Methodologically, while the current CV estimation assumes a single plane-wave front, subsequent iterations could adopt vector-based CV mapping to better capture complex propagation patterns. Finally, the observed associations with oxytocin and epidural anesthesia should be examined within a causal framework to disentangle treatment effects from underlying physiological states.

5. Conclusion

In summary, we developed a reproducible baseline framework for extracting interpretable features from multichannel EHG and for discriminating pregnancy from labor on the Icelandic 16-electrode PhysioNet dataset. Using participant-grouped validation and cost-sensitive learning, the model achieved AUROC=0.759 and AUPRC=0.319 at a sensitivity-oriented operating point. These results support the feasibility of EHG-based labor triage and provide a transparent benchmark for future work that integrates contraction-level segmentation and richer propagation/synchronization modeling.

Taken together, this work provides an interpretable and leakage-aware methodological foundation that can be extended with additional spatial features and broader validation cohorts, supporting the longer-term goal of EHG-based decision-support tools in obstetrics.

Author Contributions

The percentages of the author' contributions are presented below. The author reviewed and approved the final version of the manuscript.

	A.O.
C	100
D	100
S	100
DCP	100
DAI	100
L	100
W	100
CR	100
SR	100
PM	100
FA	100

C= concept, D= design, S= supervision, DCP= data collection and/or processing, DAI= data analysis and/or interpretation, L= literature search, W= writing, CR= critical review, SR= submission and revision, PM= project management, FA= funding acquisition.

Conflict of Interest

The author declared that there is no conflict of interest.

Ethical Consideration

Ethics committee approval was not required for this study because there was no study on animals or humans.

References

ACOG Committee. (2017). ACOG Committee Opinion No. 713: Antenatal corticosteroid therapy for fetal maturation. *Obstetrics & Gynecology*, *130*(2), e102–e109. https://doi.org/10.1097/AOG.0000000000002237

Alexandersson, Á., Sauermann, S., Gíslason, M. K., & Alexandersson, S. (2015). The Icelandic 16-electrode electrohysterogram database. *Scientific Data*, *2*, 150017.

Alexandersson, A., Steingrimsdottir, T., Terrien, J., Marque, C., & Karlsson, B. (2015). Icelandic 16-electrode electrohysterogram database (EHGDB) v1.0.0 [Data set]. PhysioNet. https://physionet.org/content/ehgdb/1.0.0/

Breiman, L. (2001). Random forests. *Machine Learning*, *45*(1), 5–32. https://doi.org/10.1023/A:1010933404324

Esgalhado, F., Batista, A. G., Vassalo, J., Castelo-Branco, M., & Henriques, J. (2020). Automatic contraction detection using uterine EHG. *Applied Sciences*, *10*(19), 7014.

Gao, H., Wen, Z., Jiang, M., Nan, Y., & Wang, Y. (2025). Enhancing uterine contraction detection through novel EHG signal processing: A pilot study leveraging the relationship between slow and fast wave components to improve signal quality and noise resilience. *Frontiers in Physiology*, *16*, 1568919. https://doi.org/10.3389/fphys.2025.1568919

Goldsztejn, U., & Nehorai, A. (2023). Predicting preterm births from electrohysterogram recordings via deep learning. *PLoS One*, *18*(5), e0285219.

Kang, J.-H., Kim, G.-Y., Lee, S.-H., & Park, J.-W. (2024). Characteristics of phase synchronization in electrohysterography for prediction of preterm birth in threatened preterm labor. *Heliyon*, *10*(22), e40433.

Lange, L., Rabotti, C., Beulen, L., Mischi, M., & Lefeber, E. (2014). Velocity and directionality of the electrohysterographic signal propagation. *PLoS One*, *9*(1), e86775.

Li, W., Yang, L., Peng, J., Du, M., Song, X., Jiang, H., & Zheng, D. (2025). Synchronization study of electrohysterography for discrimination of imminent delivery in TPL. *Computers in Biology and Medicine*, *184*, 109417.

Lucovnik, M., Kuon, R. J., Chambliss, L. R., Balducci, J., Waller, S. S., & Garfield, R. E. (2011). Use of uterine electromyography to diagnose term and preterm labor. *American Journal of Obstetrics and Gynecology*, *204*(6), 386.e1–e9.

Mas-Cabo, J., Ye-Lin, Y., Prats-Boluda, G., Garcia-Casado, J., Monfort-Ortiz, R., & Alberola-Rubio, J. (2020). Electrohysterogram for ANN-based prediction of imminent labor in TPL pregnancies. *Sensors*, *20*(9), 2681.

Mikkelsen, E., Johansen, P., Fuglsang-Frederiksen, A., & Uldbjerg, N. (2013). Electrohysterography of labor contractions: Propagation velocity and direction. *Acta Obstetricia et Gynecologica Scandinavica*, *92*(9), 1070–1078. https://doi.org/10.1111/aogs.12190

Nolte, G., Bai, O., Wheaton, L., Mari, Z., Vorbach, S., & Hallett, M. (2004). Identifying true brain interaction from EEG data using the imaginary part of coherency. *Clinical Neurophysiology*, *115*(10), 2292–2307.

Paljk Likar, I., Trojner Bregar, A., Lucovnik, M., & Geršak, K. (2022). Comparison of oxytocin vs. carbetocin uterotonic activity after cesarean section using EHG. *Sensors*, *22*(22), 8994.

Peng, J., Hao, D., Yang, L., Du, M., Song, X., Jiang, H., Zhang, Y., & Zheng, D. (2020). Evaluation of electrohysterogram measured from different gestational weeks for recognizing preterm delivery: A preliminary study using random forest. *Biocybernetics and Biomedical Engineering*, *40*(1), 352–362. https://doi.org/10.1016/j.bbe.2019.12.003

Prats-Boluda, G., Mas-Cabo, J., Ye-Lin, Y., Monfort-Ortiz, R., Alberola-Rubio, J., & Garcia-Casado, J. (2021). Optimization of imminent labor prediction systems in TPL based on EHG. *Sensors*, *21*(7), 2496.

Rabotti, C. (2010). *Characterization of uterine activity by electrohysterography* (Doctoral dissertation, Eindhoven University of Technology).

Rabotti, C., & Mischi, M. (2010). Two-dimensional estimation of the electrohysterographic conduction velocity. *Proceedings of the 32nd Annual International Conference of the IEEE EMBS*, 2470–2473.

Song, X., Yang, L., Peng, J., Du, M., Jiang, H., & Zheng, D. (2021). Automatic recognition of uterine contractions with EHG signals based on the zero-crossing rate. *Scientific Reports*, *11*(1), 1956. https://doi.org/10.1038/s41598-021-81589-3

Vandewiele, G., Dehaene, I., Kovács, G., Sterckx, L., Ongenae, F., Femont, D., Coorevits, P., Weyers, S., De Backer, G., Decruyenaere, J., Zuallaert, J., Fostier, J., & Segers, C. (2021). Overly optimistic prediction results on imbalanced data: A case study of preterm birth forecasting. *Artificial Intelligence in Medicine*, *111*, 101987.

Vasist, S. N., Prats-Boluda, G., Ye-Lin, Y., Garcia-Casado, J., Monfort-Ortiz, R., & Alberola-Rubio, J. (2022). Identification of contractions from EHG for labor evaluation. *Sensors*, *22*(6), 2070.

Vinck, M., Oostenveld, R., van Wingerden, M., Battaglia, F., & Pennartz, C. M. (2011). An improved index of phase-synchronization for electrophysiological data in the presence of volume-conduction, noise and sample-size bias. *NeuroImage*, *55*(4), 1548–1565.

Vinken, M. P. G. C., Rabotti, C., Mischi, M., & Oei, S. G. (2009). Accuracy of frequency-related parameters of the electrohysterogram for predicting preterm delivery: A review. *Obstetricial & Gynecological Survey*, *64*(8), 529–541.

Ye, Y., Alberola-Rubio, J., Garcia-Casado, J., Prats-Boluda, G., & Monfort-Ortiz, R. (2015). Effects of patient-controlled epidural analgesia on uterine EMG during labor. *Clinical and Investigative Medicine*, *38*(2), E71–E83.